Molecular Cell, Vol. 6, 139–148, July, 2000, Copyright ©2000 by Cell Press

Activation of Human Liver Glycogen Phosphorylase by Alteration of the Secondary Structure and Packing of the Catalytic Core

Virginia L. Rath, Mark Ammirati, Peter K. LeMotte, Kimberly F. Fennell, Mahmoud N. Mansour, Dennis E. Danley, Thomas R. Hynes, Gayle K. Schulte, David J. Wasilko, and Jayvardhan Pandit*
Exploratory Medicinal Sciences
Global Research and Development
Groton Laboratories
Pfizer Inc
Eastern Point Road
Groton, Connecticut 06340

Summary

Glycogen phosphorylases catalyze the breakdown of glycogen to glucose-1-phosphate, which enters glycolysis to fulfill the energetic requirements of the organism. Maintaining control of blood glucose levels is critical in minimizing the debilitating effects of diabetes, making liver glycogen phosphorylase a potential therapeutic target. To support inhibitor design, we determined the crystal structures of the active and inactive forms of human liver glycogen phosphorylase *a*. During activation, forty residues of the catalytic site undergo order/disorder transitions, changes in secondary structure, or packing to reorganize the catalytic site for substrate binding and catalysis. Knowing the inactive and active conformations of the liver enzyme and how each differs from its counterpart in muscle phosphorylase provides the basis for designing inhibitors that bind preferentially to the inactive conformation of the liver isozyme.

Introduction

Non–insulin-dependent diabetes mellitus (type 2 diabetes), estimated to affect 15 million people in the United States, is a chronic metabolic disorder characterized by defects in insulin secretion and insulin action. Type 2 diabetes can lead to serious complications such as neuropathy, nephropathy, retinopathy, premature atherosclerosis, and cardiovascular disease. Although both genetic and environmental factors have been linked to type 2 diabetes, the molecular basis of the disease remains poorly understood. However, excessive production of glucose by the liver is elevated in type 2 diabetics and is a major contributor to diabetic hyperglycemia. Recent data strongly suggest that tight blood glucose control is critical in preventing or delaying the onset of diabetic complications (Abraira et al., 1995). The liver produces glucose by gluconeogenesis (de novo synthesis of glucose) and by glycogenolysis, the breakdown of glycogen by liver phosphorylase (E.C. 2.4.1.1). Although diabetes is not caused by defects in liver phosphorylase, inhibition of this enzyme may provide a means of controlling glucose levels in circulating blood. Preliminary results have shown that inhibitors of glycogenolysis show both cellular and oral activity in reducing blood glucose levels in ob/ob mice (Hoover et al., 1998; Martin et al., 1998).

Glycogen phosphorylases catalyze the regulated phosphorolysis of an α-1, 4-glycosidic bond in glycogen to yield glucose-1-phosphate to meet the energetic needs of the cell. Glycogen phosphorylases are highly conserved from bacteria to mammals but share no homology with other carbohydrate degrading enzymes. In humans, there are three isozymes of phosphorylase that are named for the tissues in which they are predominantly expressed: liver, muscle, and brain. While the muscle and brain isozymes serve the tissues in which they are found, the role of the liver isozyme is to meet the glycemic demands of the body as a whole.

All three human isozymes are allosterically regulated by small molecule effectors and by phosphorylation of Ser-14, which cause switching between active and inactive conformations (Newgard et al., 1989). The enzyme is activated by phosphorylation (GP*a*) or by binding of AMP to the unphosphorylated form (GP*b*). In the absence of ligands, GP*b* is inactive and GP*a* may adopt the inactive conformation when ATP or glucose is bound. AMP and ATP both bind to an allosteric site distinct from either the phosphorylation site or the catalytic site, and glucose binds at the catalytic site.

Within this general framework, each human isozyme exhibits a different, tissue-specific sensitivity to allosteric effectors. In particular, the muscle and liver enzymes differ dramatically in their responses to effectors that bind to the AMP site. Overall, the human liver and human muscle proteins are 79% identical, and with one exception, all residues that bind AMP are conserved. Nonetheless, the muscle enzyme is potently and cooperatively activated by AMP while the liver enzyme is not. The unphosphorylated form of the muscle enzyme is strongly activated by AMP, to 80% of the enzyme's maximal activity, and binding is cooperative (Morgan and Parmeggiani, 1964). Binding of AMP can be competitively inhibited by ATP or Glc-6-P (Madsen, 1964; Maddaiah and Madsen, 1966; Kobayashi et al., 1982). AMP also stimulates the activity of the phosphorylated muscle enzyme by another 10% (Lowry et al., 1964; Helmreich et al., 1967). In contrast, the unphosphorylated form of the liver enzyme is inactive, shows only a slight increase in activity in the presence of AMP (10%–20%), and is insensitive to inhibition by ATP or Glc-6-P. Phosphorylation results in maximal activity that is not further increased by AMP.

The human phosphorylases exist as homodimers formed from monomers of 841 (muscle), 846 (liver), and 862 (brain) residues (Figure 1). The dimer can be thought of as having two opposite "faces." The regulatory face, containing the phosphorylation peptide and the AMP site, is exposed to the cytosol, where it can interact with the kinase, the phosphatase, and allosteric effectors. On the opposite side of the enzyme, the catalytic face is bound to the glycogen particle. Each monomer comprises an N-terminal and a C-terminal domain of about equal size. The catalytic site is formed at the domain interface. The required cofactor, pyridoxal phosphate (PLP), is attached by a covalent Schiff base linkage to Lys-680 in the C-terminal domain. The phosphorylation site, Ser-14, is contained within a region of polypeptide

*To whom correspondence should be addressed (e-mail: pandit@pfizer.com).

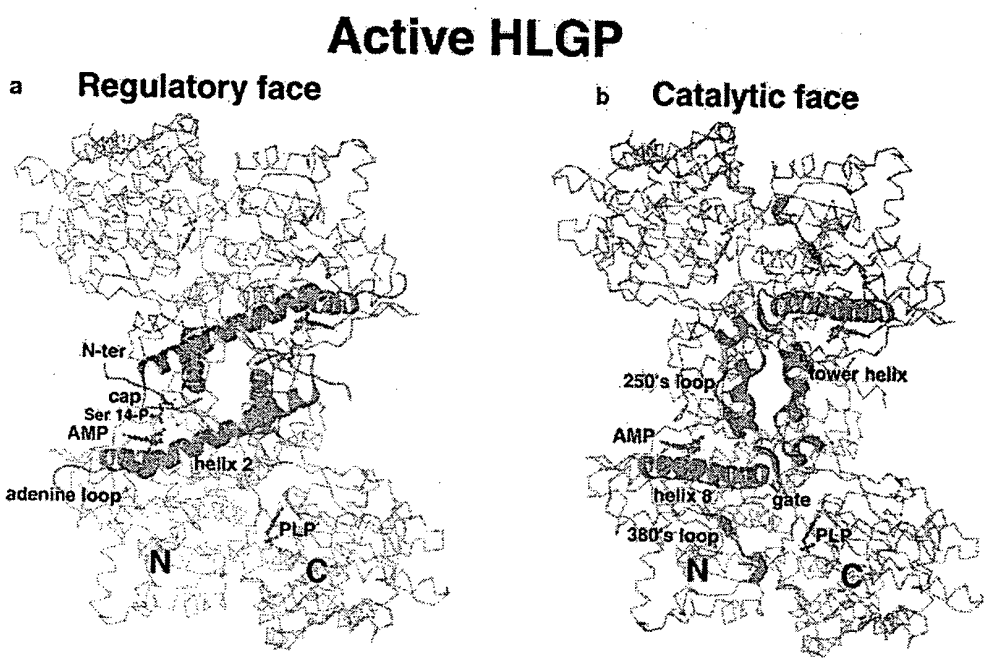

Figure 1. Overview of the Structure of Active Human Liver Glycogen Phosphorylase

Cα trace in Molscript showing key secondary structures described in the text (Kraulis, 1991). One subunit of the functional dimer is colored purple, the other gray; the N and C-terminal domains that make up each subunit are labeled. The catalytic site is marked by the cofactor, PLP.

(A) The regulatory face of the enzyme is exposed to the cytosol and includes the AMP site and the phosphorylation site. The first residue visible in the electron density map (5) is labeled N-ter. The phosphorylation site (Ser-14-P) binds across the cap (residues 42′-45′) of the AMP site. The cap is followed by helix 2 (residues 48–78), which forms the base of the AMP site and extends across the width of the protein. The cap of one AMP site leads to helix 2, which forms the base of the AMP site from the other subunit. The outside edge of the AMP site is bounded by the adenine loop, residues 315–324.

(B) The catalytic face of the enzyme is bound to the glycogen particle. The 40 residues that undergo structural rearrangement on activation are highlighted in ribbons. The 250's loop (residues 250′-260′) becomes ordered and forms a binding site for the gate (residues 280–289), whose length is shortened by extending helix 8 (residues 286–310) one turn. This shorter gate can no longer extend itself to form a binding site for the glucose analog or the 380's loop (residues 376–386). The 380's loop becomes less well ordered and moves away from the catalytic site. The tower helices (residues 267–274) from each subunit connect the 250's loop and the gate and pack together to form the heart of the subunit interface. On activation, they are shortened, and hydrogen bonds between them are lost.

that binds across the subunit interface (residues 5–22) and is referred to here as the phosphorylation peptide. Ser-14 is phosphorylated by a specific kinase, phosphorylase kinase, and is dephosphorylated by the protein phosphatase, PP1.

Here, we present the crystal structures of a human phosphorylase (Table 1). We describe the structure of the phosphorylated form of human liver glycogen phosphorylase (HLGP*a*) in its active and inactive conformations and compare them to reveal the nature of the structural transition that increases enzyme activity. The active conformation is defined by the complex of HLGP*a* with AMP, the inactive conformation by the structure of HLGP*a* complexed with a potent but nonphysiological glucose analog, *N*-acetyl-β-D-glucopyranosylamine.

The crystal structures of phosphorylases from other species are known. Rabbit muscle phosphorylase has been the subject of intensive kinetic, biochemical, and crystallographic analyses since it was first purified in the 1930's. More recently, the crystal structures of *E. coli* maltodextrin phosphorylase and GP*a* and GP*b* from *S. cerevisiae* have provided insights into the details of substrate binding and the different ways in which these enzymes are regulated by phosphorylation and by small molecules. In this report, we compare the human liver phosphorylase structures to those of the rabbit muscle, *E. coli*, and *S. cerevisiae* enzymes to reveal the dramatic changes of the catalytic core on activation and the structural basis of AMP sensitivity.

Results

Crystallization

Inactive Conformation

We cocrystallized phosphorylated human liver phosphorylase (prepared from the Baculovirus expression system) with the catalytic site inhibitor, *N*-acetyl-β-D-glucopyranosylamine (the glucose analog), in the inactive conformation of the enzyme. The glucose analog exhibits a K_i of 0.035 mM for the phosphorylated form of muscle phosphorylase, which is 50-fold lower than the K_i for α-D-glucose (1.7 mM) (Oikonomakos et al., 1995).

Active Conformation

Crystals of the active conformation were obtained as a byproduct of efforts to grow crystals of the inactive form

Table 1. Crystallographic Data and Refinement Statistics

Active			Inactive	
HLGPa/AMP, (glucose)			HLGPa/1-GlcNAc	
Space group	$P3_121$		$P3_1$	
Cell constants	a = b = 123.91 Å	c = 127.68 Å	a = b = 124.0 Å	c = 122.98 Å
	α = β = 90.0°	γ = 120.0°	α = β = 90.0°	γ = 120.0°
Asymmetric unit	monomer		dimer	
Data Collection Statistics				
Resolution	50.0 - 2.4 Å		30.0 - 2.4 Å	
Unique reflections	53,400		78,842	
Redundancy	5-6		2-3	
Resolution (last shell)	50.0 - 2.4 (2.49 - 2.4)		30.0 - 2.4 (2.49 - 2.4)	
Chi^2	1.04 (1.09)		1.17 (1.26)	
R_{merge}	0.057 (0.495)		0.047 (0.174)	
I/error	22.9 (2.2)		22.5 (5.7)	
Completeness (%)	98.5 (91.8)		99.5 (97.8)	
Refinement Statistics				
Protein	5-838		23-249, 260-316, 324-831	
Disordered	1-4, 315-324, 839-846		1-22, 250-259, 317-323, 832-846	
Ligands	AMP, (glucose)		1-GlcNAc	
Water molecules	242		255	
Resolution	50.0 - 2.4 Å (2.42 - 2.4)		30.0 - 2.4 (2.42 - 2.4)	
R	0.235 (0.353)		21.5 (29.4)	
R_{free}	0.295 (0.476)		24.9 (30.0)	
Rmsd bond lengths	0.007 Å		0.010 Å	
Rmsd bond angles	1.32°		1.93°	

Resolution, Chi^2, R_{merge}, I/error (Intensity divided by error), and completeness values taken from Scalepack results (Otwinowski and Minor, 1997). $R_{merge} = \Sigma_h\Sigma_i | I(h) - I_i(h) | / \Sigma_h\Sigma_i I_i(h)$ where $I_i(h)$ and I(h) are the ith and the mean measurement of the intensity of reflection h. $R_{cryst} = \Sigma_h [|Fobs(h) - Fcal(h)| / \Sigma_h Fobs(h)]$ where Fobs(h) and Fcal(h)| are the observed and calculated structure factor amplitudes. R_{free} is computed using 10% of the reflections from each resolution shell, randomly selected.

by different methods than those described above. In the beginning, we tried to obtain crystals of an inactive form of HLGP*a* (prepared from *E. coli* cells) by cocrystallizing with glucose (at this time the more potent glucose analog was not available), but the resulting crystals were poor. However, one preparation of the enzyme gave improved crystals, and we hypothesized that this sample contained residual AMP remaining after the AMP affinity chromatography step. Subsequently, we found that addition of glucose plus either AMP, IMP, ATP, or Glc-6-P to other preparations of the protein gave the same high-quality crystals. Because we sought to determine the complex of HLGP*a* with one of our inhibitors, we soaked the HLGP*a*/AMP/glucose crystals in solutions containing a Pfizer compound, 5-Acetyl-1-ethyl-2-oxo-2,3-dihydro-1H-indole-3-carboxylic acid (3-phenylcarbamoyl-phenyl)-amide. The resulting active state structure of human liver glycogen phosphorylase *a* contained AMP at the expected allosteric site but only weak density in the active site, suggesting poor occupancy by glucose. No density could be identified corresponding to the Pfizer compound.

Because the crystals were grown in the presence of glucose and soaked in a second inhibitor, it is possible that the conformation of the protein in the crystal is not fully active, despite the weak or absent density for the inhibitors. We think that the conformation of the protein is set by the Ser-14 phosphorylation and the presence of AMP, since AMP binds more tightly to the enzyme than glucose. The fact that glucose is not required for crystal growth and that addition of the Pfizer inhibitor to the crystallization trial actually prevents crystal growth indicates that the protein is in the active conformation. The role of the inhibitors ATP, IMP, and Glc-6-P in promoting crystal growth may be partly explained by the crystal structure of HLGP*a* with ATP, which shows that ATP is not well ordered except for the triphosphate that binds to arginines and tyrosines within the AMP site and presumably stabilizes the enzyme for crystallization (T. R. H. and V. L. R., unpublished data). Overall, the crystal structure of HLGPa/ATP is in the same active conformation described for HLGPa/AMP with some additional differences in the ATP binding site.

Overall Description of the Structures

Comparing the biologically relevant dimeric enzyme in both its inactive and active conformations reveals the structural changes that occur when the enzyme is activated and can be directly attributed to the absence of the glucose analog inhibitor. The structural changes accompanying activation can be identified by (1) order/disorder transitions, (2) calculating the root mean square difference in atomic positions for each residue (after superposition), and (3) calculating the differences in the phi and psi angles for each residue. These methods clearly identify the regions described below as key to the activation mechanism. The transition to active enzyme is defined by the refolding of the phosphorylation peptide on the regulatory face and by the repacking and, in parts, refolding, of the hydrophobic core of the enzyme on the catalytic face. The structural changes relating to the phosphorylation peptide are similar to those previously described for the rabbit muscle protein. The rearrangement of 40 residues of the catalytic core is described here in its entirety.

The Phosphorylation Peptide

Inactive Conformation

The phosphorylation peptide is completely disordered in the inactive form. No electron density is present for residues 1–23. This disorder was unexpected and suggested a novel feature in the regulation of liver phosphorylase: that the inhibited phosphorylated form was structurally identical to the unphosphorylated form. Alternatively, the missing electron density could be the result of dephosphorylation of Ser-14 or proteolysis of the N terminus during crystallization. To confirm the phosphorylation state of the protein in the crystal, protein extracted from crystals was subjected to proteolytic digestion followed by mass spectrometry of the phosphorylation peptide. From these studies, it was concluded that the HLGP*a* as prepared and derived from crystals of the glucose analog complex was phosphorylated in high yield (estimated to be greater than 80%) at Ser-14, and the absence of electron density for residues 1–23 was not due to dephosphorylation or proteolysis of the protein but rather reflected true disorder in the crystal.

Active Conformation

In the active form, the phosphorylation peptide is well ordered and stabilizes the active conformation through numerous interactions to its binding site within the subunit interface. Except for residue 21, all main chain atoms of the phosphorylation peptide are ordered, although the electron density for some side chains is weak or absent. The charge on Ser-14 phosphate is compensated by interactions with three arginines, one from the other subunit (Arg-16, Arg-43′, Arg-69; where the prime (′) indicates the second subunit). The aliphatic part of each arginine side chain also contributes to shielding the phosphate from the reach of the phosphatase. The entire phosphorylation peptide stabilizes the subunit interface by participating in numerous hydrogen bonds (mostly through backbone atoms) to residues of the second subunit within the dimer.

The Catalytic Site

Inactive Conformation

The tower helices (267–274) from each subunit are linked by hydrogen bonds (270: 274′ and 274: 270′) and form the heart of the subunit interface on the catalytic face of the enzyme. Attached to either end of the tower helix are the 250's loop (residues 250–260) and the gate (residues 280–289). Access by substrate is controlled by the concerted movement of loops at the domain interface that expose or occlude the catalytic site. The gate has previously been identified in crystal structures of rabbit muscle phosphorylase, which showed that access to the catalytic site is increased when the gate adopts an "open" position and is reduced when the gate blocks the entrance to the catalytic site in the "closed" position (Sprang et al., 1982; Acharya et al., 1991).

In the structure of human liver glycogen phosphorylase *a* in the inactive conformation, the gate is in the closed position (Figures 2A and 2C). The gate is held in place on one side by the glucose analog and on the other by the 380's loop (residues 376–386). Together, the glucose analog, gate, and 380's loop form a sandwich, filling the space between the two domains to the exclusion of substrate. The positions of both the gate and the 380's loop are further stabilized by hydrogen bonds to residues of the C-terminal domain.

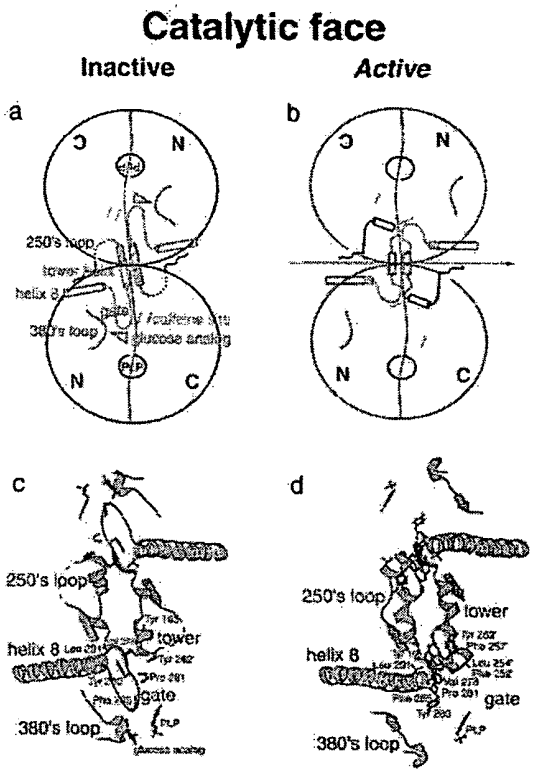

Figure 2. Refolding and Repacking the Protein Core

Cartoon showing the structural changes that occur on the catalytic face of the enzyme in the (A) inactive and active conformations of HLGP*a*. The subunits of the functional dimer are shown as circles; N, N-terminal domain; C, C-terminal domain. In the inactive structure, the caffeine site is formed but unoccupied (Phe-285 and Tyr-613 in light blue); solid red cylinder, two turn extension of the tower helix; red dotted lines, hydrogen bonds between the tower helices; dashed black lines, disordered regions of the 250's loop. In the active structure, the subunit rotation axis is shown in green; the caffeine site is absent owing to the displacement of Phe-285; helix 8 is extended by one turn (solid purple cylinder). Inactive (C) and active (D) conformations of HLGP*a* showing the secondary structural elements and ten residues identified from the structure of yeast glycogen phosphorylase that undergo rearrangement upon activation (Kraulis, 1991). Note the shortened gate and the position of Tyr-280, poised to bind substrate.

The glucose analog is well defined in the electron density and forms 12 hydrogen bonds to residues from both domains. The binding site of the glucose moiety of the analog is nearly identical to that of glucose, as seen in crystal structures of the rabbit muscle protein (Sprang et al., 1982; Martin et al., 1990). Glucose and the glucose analog differ only by their substituents at the C1 carbon with the additional N-acetyl group in the glucose analog contributing one additional hydrogen bond (to His-377) and numerous van der Waal contacts to the protein.

Through its contacts to the C-terminal domain, the gate also forms an allosteric inhibitor site, known as the purine nucleoside site, previously identified in crystal structures of rabbit muscle phosphorylase (Kasvinsky, 1978). Various heterocyclic compounds such as caffeine

have been shown to stack between the side chains of Phe-285 and Tyr-613 at this site. In doing so, these compounds act synergistically with glucose to inhibit the enzyme. In the inactive conformation described here, the aromatic rings of Phe-285 and Tyr-613 are optimally spaced to accommodate such an inhibitor.

Active Conformation

In the activated liver phosphorylase structure, the tower helix is shorter by two turns and does not form the hydrogen bonds to its mate in the other subunit, which are seen in inactive HLGP*a*. The gate is well ordered and is moved up and away from the entrance to the active site such that substrate has direct access to the catalytic residues (Figures 2B and 2D). In its open position, the gate residues make van der Waals contacts with the 250's loop of the other subunit. The length of the gate is shortened by converting part of the reverse β turn into a turn of helix, extending helix 8. This shorter gate can no longer reach to the glucose analog binding site, nor does it contact the 380's loop that is less well defined in the electron density. Main chain but not side chain atoms of the 380's loop can be built into the electron density, but the high temperature factors (79 Å^2 on average for Cα carbons) indicate that the 380's loop is quite flexible. Thus, when open, the gate contacts the 250's loop of the second subunit, and as a consequence the 380's loop of its own subunit becomes more mobile.

We did not expect to see density for glucose in the catalytic site of the active conformation, despite its presence in the crystallization drop at a concentration of 50 mM. Nonetheless, density that is most reasonably interpreted as a poorly ordered glucose molecule is present.

The AMP Binding Site

AMP is not present in the inactive conformation. In the active conformation, side chains move to improve their contacts with AMP (Figure 3A). AMP binds across the subunit interface where it is bound between a loop from one subunit termed the cap (residues 42′-45′, so called because it "caps" the AMP binding site) and a helix from the other (helix 2, residues 48–78). In the active conformation, the phosphorylated N terminus passes directly over the cap, forming both hydrogen bonds and van der Waals contacts to residues of the cap. Contacts between the phosphorylation peptide of one subunit and the cap of the other stabilize the subunit interface in the active conformation.

The Transition to Active Enzyme

Subunit Rotation

The active conformation is characterized by a rigid body rotation of the two subunits that results in an increased number of contacts between them. Compared to the inactive conformation, the hydrophobic cores of the two subunits rotate in toward each other by nearly 7 degrees (Figure 2B) (Rath and Fletterick, 1994). This rotation affects the packing and hydrogen bonds formed between the two subunits. Excluding ligands, the surface area at the subunit interface increases from 4200 to nearly 7300 Å^2, brought about by a 60% increase in van der Waals contacts. In the transition to activated enzyme, 7 hydrogen bonds unique to the inactive conformation are lost and 21 specific to the active conformation are gained.

Domain Interface Remodeled

In the active conformation, the subunit rotation is accompanied by a smaller, 1.5 degree rotation of the two domains that significantly alters the domain interface. The interface is remodeled by breaking 11 and making 8 new hydrogen bonds that are unique to the active conformation of the enzyme. The total number of hydrogen bonds formed between the two domains remains nearly constant, as does the area buried at the domain interface.

Discussion

The Phosphorylation Peptide

On the regulatory face of the enzyme, the phosphorylation peptide is disordered in the inactive conformation but ordered and bound to the surface of the protein in the active form. Its refolding and binding mode have been well characterized in the case of the rabbit muscle enzyme, and the story is essentially the same for HLGP (Sprang et al., 1988). The absence of density for the phosphorylation peptide suggests that the *inhibited phosphorylated* enzyme adopts the same conformation as expected for the *unphosphorylated* form. The inactive conformation of liver phosphorylase represents the inhibited enzyme prior to dephosphorylation by the phosphatase PP1. Releasing the phosphorylation peptide from its binding site on phosphorylase frees it to interact with the catalytic site of the phosphatase.

This structural result may explain an important difference in regulation between the two isozymes. Unlike the muscle enzyme, which is sensitive to allosteric effectors, liver phosphorylase is primarily regulated by neuronal and hormonal signals acting through the kinase and the phosphatase to alter the phosphorylation state of Ser-14. Several inactive conformations of the muscle enzyme have been identified crystallographically, apparently tuned by the occupancy of the allosteric sites. In contrast, because of its insensitivity to effectors, the liver enzyme may have only one inactive conformation, which looks like the unphosphorylated enzyme. This may be confirmed by showing that the structure of the unphosphorylated liver enzyme is identical to the inactive conformation described here.

Refolding and Repacking the Protein Core

Activation of phosphorylase by repacking the hydrophobic core was first described for yeast glycogen phosphorylase (Lin et al., 1997). In the transition from inactive to active yeast phosphorylase, 10 residues participate in a hydrophobic condensation (Figures 2C and 2D). Despite many other differences, residues that form this hydrophobic cluster of the active yeast enzyme are more conserved at the amino acid level (comparing 14 phosphorylase sequences) than those in the inactive conformation. The authors proposed that this active core would be conserved structurally in other phosphorylases. Using the human liver enzyme, we have been able to grow crystals of the active dimeric enzyme and show that the active core described in yeast phosphorylase is, in fact, preserved structurally in the liver enzyme. Conservation of this rearrangement in both yeast and liver phosphorylase at the structural (and sequence) level suggests that this activation mechanism is a general one for phosphorylases.

On activation of HLGP*a*, forty residues (residues 250–

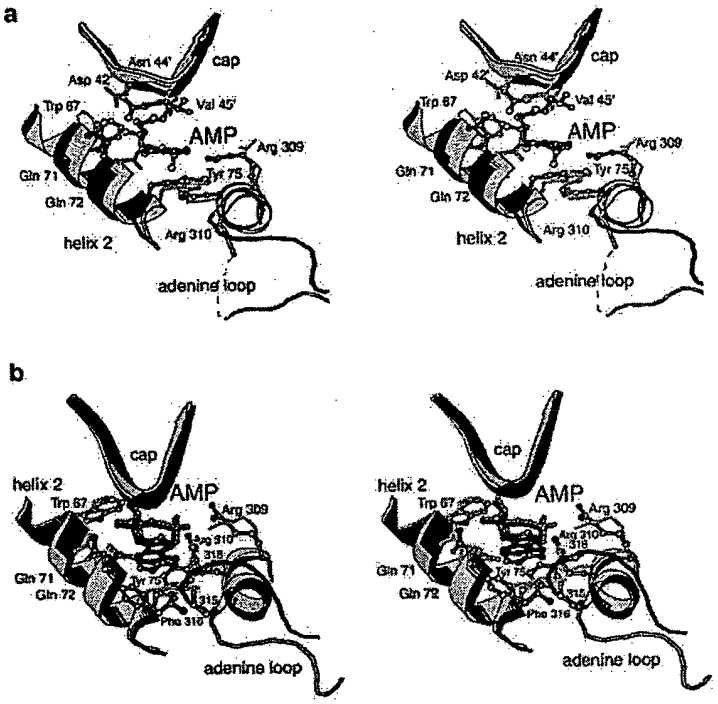

Figure 3. Differences in the Structure of the AMP Binding Site

(A) Comparison of the AMP site in inactive and active HLGP*a*. Stereo diagram of the AMP site in active liver phosphorylase (helices, strands, and coils in black; side chains and AMP represented in ball-and-stick form with atom-specific gray-scale), superimposed on the AMP site of inactive HLGP*a* (helices, strands, and coils in gray; side chains as gray sticks), made in Molscript (Kraulis, 1991).

(B) Comparison of the AMP site in muscle and liver phosphorylase. Stereo diagram of the AMP site in tetrameric RMGP*b* (helices, strands, and coils in black; side chains and AMP represented in ball-and-stick form with atom specific gray-scale [Sprang et al., 1991]), superimposed on the AMP site of active HLGP*a* (helices, strands, and coils in gray, side chains as gray sticks, and AMP represented as black ball-and-stick), made in Molscript (Kraulis, 1991). Residues 42', 44', and 45' of the cap that form hydrogen bonds and van der Waals contacts to AMP in both structures are omitted for clarity. In muscle phosphorylase, the adenine N6 amino group is specified by the main chain carbonyls of residues 315, 318, and the side chain of Phe-316.

290, equivalent to the 250's loop, tower, and gate) undergo either order or disorder transitions, changes in secondary structure, and/or repacking, resulting in a larger subunit interface with new hydrogen bonds and van der Waals contacts. The two subunits rotate toward each other and lock into a register that reorganizes the catalytic site for substrate binding and catalysis. The conformation of the 250's loop and gate are virtually identical in the crystal structures of active liver and yeast phosphorylase. In addition, all 10 of the side chains identified as part of the hydrophobic cluster in yeast phosphorylase are found in virtually identical positions in the *active* HLGP*a* structure (Figure 2D). In contrast, the positions of these residues in the *inactive* structures of liver, muscle, and yeast phosphorylase are quite different (Acharya et al., 1991; Rath, 1991).

Changes in the tower and gate in active HLGP*a* also prepare the catalytic core for substrate binding and catalysis. Recent crystallographic studies on maltodextrin phosphorylase (MalP) from *E. coli* have revealed the substrate binding site of the glycogen polymer in phosphorylase (Watson et al., 1999), and we find that many of the substrate binding residues are correctly placed in active HLGP*a*. Arg-569 and Lys-574 are positioned to bind phosphate (Goldsmith et al., 1989; Watson et al., 1999), with Tyr-280, Asp-339, Lys-568, His-571, and Tyr-613 placed to bind the glucose polymer. Of the residues that bind substrate, only the 380's loop is out of place. Relative to its position in the MalP complex, the 380's loop is pushed away from its position in the bound conformation, making it solvent exposed.

Loss of AMP Activation and Cooperative Binding in Liver Phosphorylase

In muscle phosphorylase, AMP stabilizes the active conformation of the enzyme by binding across the subunit interface between the cap of one subunit and helix 2 of the other. Thus, the cap of the AMP binding site from one subunit extends into helix 2 at the base of the AMP binding site from the second subunit. The importance of stabilizing this part of the subunit interface for activation was demonstrated by creating a metal binding site between the cap and helix 2 and showing that activity increased in the presence of metals bound to the site (Browner et al., 1994). The stabilized tight subunit interface is linked to structural changes at the catalytic site that increase enzyme activity (Sprang et al., 1987).

Despite the conservation of binding site residues, many of the interactions with AMP seen in muscle phosphorylase are absent in the complex of the liver enzyme with AMP (Figures 4A and 4B). The loss of contacts to binding site residues is primarily the result of a rigid body rotation between the two subunits and, secondarily, due to alterations in side chain positions. The rotation of the subunits with respect to each other increases the distance between Cα carbons of the cap and helix 2 by 0.5 Å (on average), and five hydrogen bonds seen in the muscle phosphorylase/AMP complex are lost. The remaining ionic and stacking interactions are similar to those in muscle phosphorylase.

In the muscle enzyme, AMP also contacts a surface loop termed the adenine loop (residues 315–325, Figure 4A). In muscle phosphorylase, the adenine N6 amino group is specified (over inosine) by the main chain carbonyls of residues within this loop (Sprang et al., 1991). These contacts are absent in the liver phosphorylase complex because the loop adopts a different conformation (Figure 3B). Although the adenine loop is poorly ordered in active HLGP*a*, the path of the main chain can be modeled with confidence. As modeled, the adenine loop does not adopt the conformation seen in the muscle enzyme, because of steric overlap with Tyr-75 and because several hydrogen bonds that stabilize the conformation observed in the muscle structure are absent due

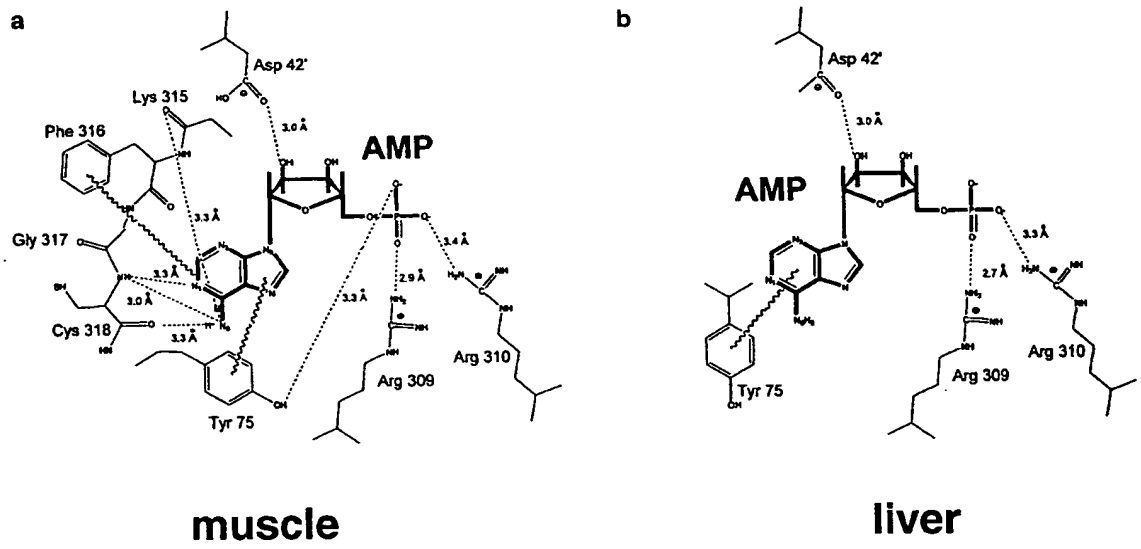

Figure 4. Contacts between AMP and Phosphorylase

(A) Interactions between Muscle phosphorylase and AMP. Chemdraw figure (CambridgeSoft, 1999) showing the hydrogen bonds and principal van der Waals contacts (3.4-4.2 Å, wavy lines) between AMP and tetrameric rabbit muscle phosphorylase *b* (Sprang et al., 1991).
(B) Interactions between HLGP*a* and AMP. Chemdraw figure (CambridgeSoft, 1999) showing the hydrogen bonds and principal van der Waals contacts between AMP and active HLGP*a*.

to sequence changes. The flexibility of the adenine loop is likely due to the fact that it is solvent exposed and forms no contacts to the body of the protein.

We propose that the loss of AMP cooperative binding and weak enzyme activation in the liver isozyme results from changes at the subunit interface, notably in the conformation of the adenine loop. The adenine loop connects the AMP site to the active site gate through helix 8 (Figure 1). Without the contacts between AMP and the adenine loop, the effect of AMP binding may not be coupled to the active site (as previously proposed [Kobayashi et al., 1982]). The loss of cooperative binding in liver phosphorylase may be due to the fact that AMP forms fewer hydrogen bonds to residues of helix 2. Cooperative binding of AMP in muscle phosphorylase is propagated through helix 2 to the other subunit (Figure 1).

In addition to the adenine loop, other residues of the subunit interface in human liver phosphorylase may also play a part in the altered AMP response. A chimeric phosphorylase consisting of the first 48 residues of the human muscle sequence followed by the rest of the liver isozyme (a total of 10 amino acid changes) could be activated by AMP and exhibited a higher specific activity than the wild-type liver enzyme, although its affinity for AMP was unchanged (Coats et al., 1991). There are significant differences in the intersubunit hydrogen bonds for residues 5–48 comparing the rabbit muscle and human liver crystal structures. Though none are the result of sequence changes, this suggests that regions of the subunit interface outside of the AMP binding site are also important for activation by AMP.

Comparison of the Activation Mechanisms of Human Liver Phosphorylase and Rabbit Muscle Phosphorylase

The mechanism of enzyme activation in human liver and rabbit muscle phosphorylase (RMGP) is expected to be conserved. A strict comparison cannot be made because of the lack of a fully activated, dimeric, muscle phosphorylase crystal structure. In all the RMGP structures solved to date, the enzyme is either inhibited in some way or forms a tetramer in which the catalytic site is blocked. The 250's loop, a key part of the hydrophobic condensation, is disordered in all known muscle phosphorylase structures. The fact that yeast phosphorylase and HLGP (49% identical at the amino acid level) share the same activation mechanism strongly suggests that the more closely related mammalian phosphorylases (80% sequence identity between human liver and rabbit muscle phosphorylase) are also activated in the same way.

A comparison of the inactive and active conformations of HLGP and RMGP shows that in both enzymes, the solvent accessible surface area of the subunit is decreased (by 3100 and 2220 Å^2, respectively) when the enzyme is activated and hydrogen bonds that are specific for the inactive conformation are replaced by a greater number of hydrogen bonds that are specific for the active conformation. About half of the conformation-specific hydrogen bonds are found in both RMGP and HLGP; the remainder are isozyme specific. Activation of both isozymes involves a larger subunit rotation (about a conserved axis) and smaller domain rotation, similar in magnitude.

The tissue-specific functional differences between liver and muscle phosphorylase result from differences in the subunit interface and not from alterations in residues that bind ligands. This result was unanticipated because of the high sequence conservation of interface residues. Of the residues forming the subunit interface in rabbit muscle phosphorylase, there are only three amino acid differences in the human liver sequence (Rath et al., 1987). Changes in the relative orientation of the hydrophobic cores of the subunits and in the hydrogen bonds and van der Waals contacts between

the subunits cause a repacking of the subunit interface. This repacking creates a liver phosphorylase dimer that is distinct from that of the muscle enzyme and could not have been predicted by sequence comparison.

Knowing the atomic resolution structure of the inactive and active forms of HLGP*a* provides us with the necessary background to design inhibitors that preferentially stabilize the inactive conformation of the liver enzyme. Inhibitors (binding at either the active site or the allosteric sites) can be optimized to maximize direct contact to the inactive conformation and to avoid contacts to the active conformation of the enzyme. A further goal, which may be critical for obtaining an effective drug, is to identify compounds that are selective inhibitors of the liver isozyme. Inhibition of muscle or brain phosphorylase could lead to unwanted side effects over the lifetime of treatment most diabetics require. Comparative structural studies of the human liver, muscle, and brain phosphorylases have been initiated to address this issue.

Experimental Procedures

Expression

HLGP (cDNA from R. J. Fletterick, UCSF) was originally expressed in *E. coli*, and later a Baculovirus system was used due to improved expression. In *E. coli*, the protein was expressed from plasmid pKK233-2 (Pharmacia) in strain XL-1 Blue (Stratagene). The strain was inoculated into LB medium (plus 100 mg/L ampicillin, 100 mg/L pyridoxine, and 600 mg/L $MnCl_2$), grown at 37°C to a cell density of OD_{550}= 1.0, and induced for 3 hr with 1 mM isopropyl-1-thio-β-D-galactoside (IPTG) prior to harvest. In SF9 insect cells, the HLGP cDNA was expressed from plasmid pBlueBac III (Invitrogen) cotransfected with BaculoGold Linear Viral DNA (Pharmingen). Cells were grown in SF900 II media (GIBco-BRL) at 27°C under serum free conditions at a multiplicity of infection of 0.5 for 22 hr and at a cell density of 2 × 10^6 cells/ml and harvested after 72 hr.

Preparation of Cell Lysate

The *E. coli* cells were resuspended in lysis buffer (25 mM β-glycerophosphate [pH 7.0], containing 0.2 mM DTT, 1 mM $MgCl_2$, 0.7 μg/ml Pepstatin A, 0.5 μg/ml Leupeptin, 0.2 mM phenylmethylsulfonyl fluoride (PMSF), and 0.5 mM EDTA), treated with 200 μg/ml lysozyme, 3 μg/ml DNAase, and 10 mM $MgCl_2$, and sonicated. The lysate was clarified by centrifugation at 35,000 × g for 1 hr. Infected SF-9 cells were resuspended in lysis buffer (0.1 M β-glycerophosphate [pH 7.5], containing 0.15 M NaCl, 1 μg/ml Pepstatin A, 1 μg/ml Leupeptin, and 1 mM PMSF) treated with 3 μg/ml DNAase and 10 mM $MgCl_2$, followed by sonication on ice. The lysate was clarified by centrifugation at 40,905 × g for 50 min.

Purification of HLGP from *E. coli*

HLGP in the soluble fraction of the lysate was purified by immobilized Cu^{+2} affinity chromatography, 5′-AMP-Sepharose chromatography, Green A dye-ligand chromatography, phosphorylation to HLGP*a* using phosphorylase kinase, and Mono Q chromatography.

Purification of HLGP from SF9 Cells

HLGP in the soluble fraction of the SF9 lysate was purified by immobilized Cu^{+2} affinity chromatography, phosphorylation to HLGP*a* using phosphorylase kinase, and Mono Q chromatography.

Cu^{+2} Affinity Chromatography

Phosphorylase can be purified on metal affinity columns without a histidine tag (Luong et al., 1992). Chelating Sepharose Fast Flow (Pharmacia) was charged with 0.1 M $CuCl_2$ and washed with buffer A (20 mM β-glycerophosphate [pH 7.5], 0.3 M NaCl, 0.2 mM DTT, 1 μg/ml Pepstatin A, 1 μg/ml Leupeptin, and 2 mM imidazole) followed by buffer B (buffer A + 0.1 M imidazole [pH 7.5]). Lysate was diluted with buffer A plus 0.2 M NaCl and 2 mM imidazole, loaded onto the column, and eluted using a 0–40 mM imidazole gradient.

5′-AMP-Sepharose Chromatography

The desalted pool from the Cu^{+2} metal affinity step was mixed with 70 ml of 5′-AMP Sepharose equilibrated with buffer C (25 mM Tris-HCl [pH 7.3] and 3 mM DTT), agitated for 1 hr at 22°C, packed into a column, washed, and eluted with buffer D (25 mM Tris-HCl [pH 7.3], 0.2 mM DTT, and 10 mM AMP). HLGP containing fractions were pooled and dialyzed into buffer E (25 mM β-glycerophosphate [pH 7.0], 0.2 mM DTT, 0.3 mM EDTA, and 200 mM NaCl).

Dye-Ligand Affinity Chromatography

The dialyzed fractions from the 5′-AMP-Sepharose column were loaded onto a Matrex Green A agarose column (Amicon) equilibrated with buffer E and eluted with buffer E plus 20 mM 5′-AMP.

Phosphorylation of HLGP*b*

Beads (AffiGel 10, BioRad) of immobilized phosphorylase kinase (Sigma) were equilibrated with kinase buffer (25 mM β-glycerophosphate [pH 7.5], 0.5 mM EDTA, 0.25 mM DTT, 1 μg/ml Pepstatin A, 1 μg/ml Leupeptin, 1 mM PMSF, and 0.02% NaN_3) and resuspended with the dialyzed Cu^{2+} affinity step pool. 7 mM ATP and 22 mM $MgCl_2$ were added, the suspension agitated at room temperature for 2 hr, transferred to a column, and washed with kinase buffer. Conversion to the phosphorylated enzyme was monitored by isoelectric focusing. In preparation for anion exchange chromatography, the pool was dialyzed against 20 mM Tris-HCl (pH 7.5), 0.5 mM EDTA, 0.25 mM DTT, 1 μg/ml Pepstatin A, 1 μg/ml Leupeptin, and 1 mM PMSF.

Anion Exchange Chromatography

Dialyzed HLGP*a* was loaded onto a Resource Q or Mono Q column previously equilibrated in buffer F (20 mM Tris/HCl [pH 7.5], 1 mM EDTA, 0.5 mM DTT, 1 μg/ml Pepstatin A, and 1 μg/ml Leupeptin) and eluted using a linear gradient to 0.3 M NaCl. Fractions were pooled, dialyzed against 50 mM NaBES (pH 6.8), 1 mM EDTA, 0.5 mM DTT, 4 mM NaCl, and 0.02% NaN_3 and assayed for activity (Rath et al., 1992).

Crystallization of the Inactive Conformation

Baculovirus derived HLGP*a* was concentrated to 20–40 mg/ml in 20 mM NaBES (pH 6.8), 1 mM EDTA, and 0.5 mM DTT. After concentration, 30–80 mM *N*-acetyl-β-D-glucopyranosylamine was added. Hanging drops were made with equal volumes of the complex and reservoir solution (0.1 M NaMES [pH 6.0] and 25%–35% MPD), and crystals were grown at 17°C.

Crystallization of the Active Conformation

E. coli derived HLGP*a* was concentrated to 10–20 mg/ml in 20 mM NaBES (pH 6.8), 1 mM EDTA, 0.5 mM DTT, 50 mM glucose, and a 4:1 molar excess of AMP. Hanging drops were made with equal volumes of the complex and reservoir solution (0.1 M Tris-HCl [pH 8.5] and 12% PEG 8000) and crystals were grown at room temperature. Before data collection, crystals were soaked overnight in a cryoprotective solution, of 20% glycerol, 80% well solution and 1 mM of an inhibitor [5-Acetyl-1-ethyl-2-oxo-2,3-dihydro-1H-indole-3-carboxylic acid (3-phenylcarbamoyl-phenyl)-amide; Pfizer, Inc., Groton, CT; experimental details to be published separately]. This compound has an IC_{50} for HLGP*a* of 122 nM in the presence of 7.5 mM glucose.

Data Collection and Structure Solution

Prior to data measurement, the crystals were flash frozen in a nitrogen gas stream at 100°K directly from the drop. Data were measured either on an R-Axis II or a MAR 30 cm image plate detector using Cu Kα X-rays from a Rigaku generator operating at 50 kv and 100 mA. All data were processed using DENZO and SCALEPACK (Otwinowski and Minor, 1997). Refinement was carried out using iterative cycles of manual refitting in O (Jones et al., 1991), simulated annealing "omit" refinement, torsional dynamics, or conjugate gradient least squares refinement in X-*PLOR* (Brunger, 1992) or CNS (Brunger et al., 1998). The active crystal form was solved by molecular replacement using the coordinates of the phosphorylated form of RMGP (1GPA) as a search model in Amore (Navaza, 1994). The inactive conformation was solved using the refined coordinates of

the active conformation as a starting model in X-*PLOR* (Brunger, 1992). Several errors in the amino acid sequence (Newgard et al., 1986) were identified by resequencing the entire cDNA (M. Carty, W. Soeller, GenBank AF066858).

Digest of HLGP*a*

HLGP*a*, which had not been crystallized, was desalted by RP-HPLC (Geoghegan, 1996) and dried in a SpeedVac concentrator. The dried protein was redissolved in 0.4 M NH_4HCO_3, 8 M urea, and 7.5 mM DTT, incubated at 37°C for 30 min, and treated with 14 mM iodoacetamide at 22°C for 15 min. The sample was diluted to a final concentration of 0.1 M NH_4HCO_3, and 2 M urea and digested for 18 hr at 37°C with lysyl endopeptidase (Wako) (Stone and Williams, 1993).

Digest of HLGP*a*

Crystalline HLGP*a* was dissolved in 0.4 M NH_4HCO_3 and 8 M urea, desalted by RP-HPLC, dried, and digested as above using both lysyl endopeptidase and endoproteinase Glu-C (Roche Molecular Biochemicals).

Liquid Chromatography-Mass Spectrometry

Liquid chromatography-mass spectrometry (LC-MS) was conducted on a Hewlett-Packard Model 1090 HPLC connected through a Finnigan electrospray interface to a Finnigan LCQ ion-trap mass spectrometer. Peptide mapping of proteolytic digests was accomplished using a 1.6%–50% acetonitrile gradient applied to a Vydac C18 narrowbore column. A Lys-C digest of HLGP*a*, which had not been crystallized, was analyzed by LC-MS. Several mass spectra corresponding to the phosphopeptide (RRQIpSIRGIVGVENVAELK, expected mass = 2217.5 Da) were observed, consisting of MH_3^{3+} = 740.1 and MH_2^{2+} = 1109.9. MS/MS of both species gave spectra dominated by two strong peaks; at m/z = 707.5 for MH_3^{3+} and at m/z = 1060.6 for MH_2^{2+}, each of which corresponds to loss of 98 Da (elimination of H_3PO_4 from serine to produce hydroalanine) from the multiply charged ion. Low-level signals corresponding to fragmentation of the MH_2^{2+} ion confirmed the expected sequence. As this sequence contains only one hydroxyamino acid residue, phosphorylation could only have been at Ser-14. A similar analysis was then conducted on a digest of HLGP*a* from crystals of the glucose analog complex. The presence of the phosphopeptide (the Lys-C fragment discussed above, obtained without cleavage at the internal glutamate) in this material was confirmed by detecting the same three-scan fingerprint, including narrow-range scanning and MS/MS of its MH_2^{2+} ion. No significant m/z peaks corresponding to the predicted MH_3^{3+} or MH_2^{2+} ions of the unphosphorylated form of the peptide (residues 10–28, predicted mass = 2137.5 D) were detected in the LC-MS data, suggesting that the unphosphorylated peptide was either absent or a minor contaminant.

Acknowledgments

Sincere thanks to L. N. Johnson and G. W. Fleet for *N*-acetyl-β-D-glucopyranosylamine; to K. A. Watson and L. N. Johnson for the coordinates of the *E. coli* MalP complex; to Lise Hoth and Kieran F. Geoghegan (Protein Chemistry, Global Research and Development, Groton Laboratories) for determination of the phosphorylation state of the protein in the crystals; and to J. L. Treadway and D. J. Hoover for their support and encouragement.

Received February 3, 2000; revised May 2, 2000.

References

Abraira, C., Colwell, J.A., Nuttall, F.Q., Sawin, C.T., Nagel, N.J., Comstock, J.P., Emanuele, N.V., Levin, S.R., Henderson, W., and Lee, H.S. (1995). Veterans affairs cooperative study on glycemic control and complications in type II diabetes (VA CSDM). Results of the feasibility trial. Veterans affairs cooperative study in type II diabetes. Diabetes Care *18*, 1113–1123.

Acharya, K.R., Stuart, D.I., Varvill, K.M., and Johnson, L.N. (1991). Glycogen Phosphorylase *b*: Description of the Protein Structure (Teaneck, New Jersey: World Scientific Publishing).

Browner, M.F., Hackos, D., and Fletterick, R.J. (1994). Identification of the molecular trigger for allosteric activation in glycogen phosphorylase. Nat. Struct. Biol. *1*, 327–333.

Brunger, A.T. (1992). *X-PLOR* Manual. Version *3*, 1.

Brunger, A.T., Adams, P.D., Clore, G.M., DeLano, W.L., Gros, P., Grosse-Kunstleve, R.W., Jiang, J.-S., Kuszewski, J., Nilges, M., Pannu, N.S., et al. (1998). Crystallography and NMR system; a new software suite for macromolecular structure determination. Acta Crystallogr. D *54*, 905–921.

CambridgeSoft (1999). ChemDraw Pro (Cambridge, MA: CambridgeSoft).

Coats, W.S., Browner, M.F., Fletterick, R.J., and Newgard, C.B. (1991). An engineered liver glycogen phosphorylase with AMP allosteric activation. J. Biol. Chem. *266*, 16113–16119.

Geoghegan, K.F. (1996). Modification of amino groups. In Current Protocols in Protein Science, J.E. Coligan, B.M. Dunn, H.L. Ploegh, D.W. Speicher, and P.T. Wingfield, eds. (New York: John Wiley), pp. 15.2.1–15.2.18.

Goldsmith, E.J., Sprang, S.R., Hamlin, R., Xuong, N.-H., and Fletterick, R.J. (1989). Domain separation in the activation of glycogen phosphorylase *a*. Science *245*, 528–532.

Helmreich, E., Michaelides, M.C., and Cori, C.F. (1967). Effects of substrates and a substrate analog on the binding of 5′-adenylic acid to muscle phosphorylase (a). Biochemistry *6*, 3695–3710.

Hoover, D.J., Lefkowitz-Snow, S., Burgess-Henry, J.L., Martin, W.H., Armento, S.J., Stock, I.A., McPherson, R.K., Genereux, P.E., Gibbs, E.M., and Treadway, J.L. (1998). Indole-2-carboxamide inhibitors of human liver glycogen phosphorylase. J. Med. Chem. *41*, 2934–2938.

Jones, T.A., Zou, J.-Y., Cowan, S.W., and Kjeldgaard, M. (1991). Improved methods for building protein models in electron density maps and the location of errors in these models. Acta Crystallogr. A *47*, 110–119.

Kasvinsky, P.J., Madsen, N.B., Sygusch, J., and Fletterick, R.J. (1978). The regulation of glycogen phosporylase *a* by nucleotide derivatives. Kinetic and X-ray crystallographic studies. J. Biol. Chem. *253*, 3343–3351.

Kobayashi, M., Soman, G., and Graves, D.J. (1982). A comparison of the activator sites of liver and muscle glycogen phosphorylase *b*. J. Biol. Chem. *257*, 14041–14047.

Kraulis, P. (1991). Molscript—a program to produce both detailed and schematic plots of protein structures. J. Appl. Cryst. *24*, 946–950.

Lin, K., Hwang, P.K., and Fletterick, R.J. (1997). Distinct phosphorylation signals converge at the catalytic center in glycogen phosphorylases. Structure *5*, 1511–1523.

Lowry, O.H., Schulz, D.W., and Passonneau, J.V. (1964). Effects of adenylic acid on the kinetics of muscle phosphorylase *a*. J. Biol. Chem. *239*, 1947–1953.

Luong, C.B.H., Browner, M.F., Fletterick, R.J., and Haymore, B.L. (1992). Purification of glycogen phosphorylase isozymes by metal affinity chromatography. J. Chromatogr. *584*, 77–84.

Maddaiah, V.T., and Madsen, N.B. (1966). Kinetics of purified liver phosphorylase. J. Biol. Chem. *241*, 3873–3881.

Madsen, N.B. (1964). Allosteric properties of phosphorylase *b*. Biochem. Biophys. Res. Comm. *15*, 390–395.

Martin, J.L., Johnson, L.N., and Withers, S.G. (1990). Comparison of the binding of glucose and glucose 1-phosphate derivatives to T-state glycogen phosphorylase *b*. Biochemistry *29*, 10745–10757.

Martin, W.H., Hoover, D.J., Armento, S.J., Stock, I.A., McPherson, R.K., Danley, D.E., Stevenson, R.W., Barrett, E.J., and Treadway, J.L. (1998). Discovery of a human liver glycogen phosphorylase inhibitor that lowers blood glucose in vivo. Proc. Natl. Acad. Sci. USA *95*, 1776–1781.

Morgan, H.E., and Parmeggiani, A. (1964). Regulation of glycogenolysis in muscle. J. Biol. Chem. *239*, 2440–2445.

Navaza, J. (1994). AMoRe: an automated package for molecular replacement. Acta Crystallogr. A *50*, 157–163.

Newgard, C.B., Nakano, K., Hwang, P.K., and Fletterick, R.J. (1986). Sequence analysis of the cDNA encoding human liver glycogen

phosphorylase reveals tissue-specific codon usage. Proc. Natl. Acad. Sci. USA *83*, 8132–8136.

Newgard, C.B., Hwang, P.K., and Fletterick, R.J. (1989). The family of glycogen phosphorylases: structure and function. Crit. Rev. Biochem. Mol. Biol. *24*, 69–99.

Oikonomakos, N.G., Kontou, M., Zographos, S.E., Watson, K.A., Johnson, L.N., Bichard, C.J.F., Fleet, G.W.J., and Acharya, K.R. (1995). *N*-acetyl-β-D-glucopyranosylamine: a potent T-state inhibitor of glycogen phosphorylase. A comparison with α-D-glucose. Protein Sci. *4*, 2469–2477.

Otwinowski, Z., and Minor, W. (1997). Processing of X-ray diffraction data collected in oscillation mode. Methods Enzymol. *276*, 307–326.

Rath, V.L. (1991). Allosteric Mechanisms in Phosphorylases. Ph. D. thesis, University of California, San Francisco, San Francisco, California.

Rath, V.L., and Fletterick, R.J. (1994). Parallel evolution in two homologues of phosphorylase. Nat. Struct. Biol. *1*, 681–690.

Rath, V.L., Newgard, C.B., Sprang, S.R., Goldsmith, E.J., and Fletterick, R.J. (1987). Modeling the biochemical differences between rabbit liver phosphorylase. Proteins *2*, 225–235.

Rath, V.L., Hwang, P.K., and Fletterick, R.J. (1992). Purification and crystallization of glycogen phosphorylase from *Saccharomyces cerevisiae*. J. Mol. Biol. *225*, 1027–1034.

Sprang, S.R., Goldsmith, E.J., Fletterick, R.J., Withers, S.G., and Madsen, N.B. (1982). Catalytic site of glycogen phosphorylase: structure of the T state and specificity for α-D-Glucose. Biochemistry *21*, 5364–5371.

Sprang, S., Goldsmith, E., and Fletterick, R. (1987). Structure of the nucleotide activation switch in glycogen phosphorylase *a*. Science *237*, 1012–1019.

Sprang, S.R., Acharya, K.R., Goldsmith, E.J., Stuart, D.I., Varvill, K., Fletterick, R.J., Madsen, N.B., and Johnson, L.N. (1988). Structural changes in glycogen phosphorylase induced by phosphorylation. Nature *336*, 215–221.

Sprang, S.R., Withers, S.G., Goldsmith, E.J., Fletterick, R.J., and Madsen, N.B. (1991). Structural basis for the activation of glycogen phosphorylase *b* by adenosine monophosphate. Science *254*, 1367–1371.

Stone, K.L., and Williams, K.R. (1993). Enzymatic digestion of proteins and HPLC peptide isolation. In A Practical Guide to Protein and Peptide Purification for Microsequencing, P. Matsudaira, ed. (San Diego: Academic Press), pp. 43–69.

Watson, K.A., McCleverty, C., Geremia, S., Cottaz, S., Driguez, H., and Johnson, L.N. (1999). Phosphorylase recognition and phosphorolysis of its oligosaccharide substrate: answers to a long outstanding question. EMBO J. *18*, 4619–4632.

Protein Data Bank ID Codes

The coordinates of the active and inactive crystal structures of human liver phosphorylase *a* will be deposited in the Protein Data Bank.